

Mechanical Behavior of TWIP Steel in High Strain Rate Torsional Test

A. Khosravifard^{1*}, M. M. Moshksar² and R. Ebrahimi³

Department of Materials Science and Engineering, School of Engineering, Shiraz University, Shiraz 71348, Iran

Abstract

Advanced high strength steels (AHSS) have recently attracted great attention because of their superior mechanical properties. A modern group of these steels, known as twinning induced plasticity (TWIP) steels, shows a unique combination of strength and ductility even at high rates of strain. In order to examine the functionality of such steels in dynamic loading conditions, their mechanical behavior should be characterized by high strain rate experiments. Regarding the precision of its results and characteristics of the loading pulse, the torsional Kolsky bar experiment has well-known advantages over similar high rate experiments. In this study, a high strain rate torsional testing machine was designed and constructed. By using high strain rate torsional experiments in the range of strain rates from 500 to 1700 /s, mechanical behavior of two high manganese steels with different levels of carbon (0.49 and 0.07 wt%) was surveyed. Through the experiments, it was observed that the phenomenon of adiabatic temperature rise considerably decreased the work hardening rate during the dynamic testing of the high-carbon steel, whereas the low-carbon steel showed a definitely higher hardening rate. The influence of pre-straining on the dynamic mechanical behavior of this low-carbon steel was also studied.

Keywords: High strain rate, Torsional test, High manganese steel, pre-strain.

1. Introduction

There exist numerous areas of application for materials at high rates of strain. One of the well-known examples of tolerating impact loads is a car body in the instance of a crash. In order to improve the safety conditions, it must be constructed from a material with sufficient crashworthiness¹⁾. Inevitably, the candidate materials for such applications must be characterized at the same high strain rate of their intended application. Various methods for high strain rate testing of materials have been introduced after the original work of John Hopkinson²⁾. In order to examine the ductile materials at dynamic loading conditions, Kolsky³⁾ invented his so-called Hopkinson pressure bar. After about a decade, high rate tensile experiments were conducted by introducing some variations in the Hopkinson pressure bar technique⁴⁾. Finally, Baker and Yew⁵⁾ were the first who extended the Hopkinson experiments to torsional state of stress.

Due to their superior mechanical properties, advanced high strength steels (AHSS) have been the subject of numerous recent research works. A modern sub-category of these steels, i.e. twinning

induced plasticity (TWIP) steels, possesses an excellent combination of strength and ductility. More interestingly, favored mechanical properties of TWIP steels are maintained up to high ranges of strain rate⁶⁾. Consequently, such steels have been recently considered as suitable candidates for car body structures. Usually, a high manganese content of 15-30 wt% exists in the composition of the steel, so that the austenite phase is preserved down to room temperature. In addition, some aluminum and silicon may also be added to control the stacking fault energy (SFE) of the steel. The former leads to an increase and the latter to a decrease of SFE. The value of this energy must be adjusted in the range of 15-35 mJ/m² so that mechanical twinning would be the dominant deformation mechanism⁷⁾. Mechanical twins act as obstacles against the moving dislocations and consequently, increase the work hardening capability of the steel. This prevents the localization of strain and leads to high ductility for these high-Mn steels⁸⁾. Numerous research works on the microstructural features of TWIP steels and their mechanical properties have been thoroughly reviewed by Bouaziz et al.⁹⁾. However, in these recent studies, the mechanical behavior of high-Mn steels at high rates of strain, especially with a torsional state of stress, has rarely been investigated. In the present work, a high strain rate torsional testing machine was firstly designed and constructed. Subsequently, two high manganese steels with quite different concentrations of carbon (0.49 and 0.07 wt.%) were tested by the constructed machine. The effect of pre-straining on the successive high-rate straining of the steel was also studied.

* Corresponding author:

Tel: +98 917 7031636

Fax: +98 711 2307293

Email: akhosravi@shirazu.ac.ir

Address: Department of Materials Science and Engineering,
School of Engineering, Shiraz University, Shiraz 71348, Iran

1. Ph.D. Student

2. Professor

3. Associate Professor

2. Designing the Machine and the Experimental Procedure

High strain rate torsional experiment is more costly when compared to the compressive version of the experiment. However, accuracy and precision of the results obtained from the torsional experiment are higher than those of the compressive test¹⁰. A schematic representation of the torsional test setup designed and constructed in the present work is shown in Figure 1.

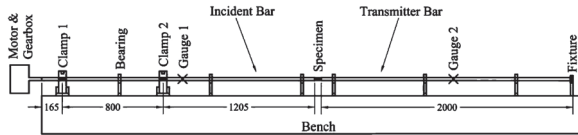


Fig. 1. Schematic representation of the torsional testing setup used in the present study (dimensions in mm).

In order to perform a test, the incident bar was fixed by clamp 2, while the end of the bar was twisted by the motor and gearbox to a desired angle. Thus, a specific amount of torque was stored between the gearbox and clamp 2. At this moment, clamp 1 fixed the bar and clamp 2 was suddenly released by fracturing its notched pin. As a result, half of the stored torque traveled towards the specimen and the other half towards clamp 1. This clamp reflected the torsional pulse, and hence prevented damage to the motor and gearbox system. On the other hand, a part of the torque which crashed the specimen was reflected back to the incident bar, whereas another part was transmitted into the so-called transmitter bar. Values of the generated strains on the surface of the incident and transmitter bars were continuously measured by gauges 1 and 2, respectively. Each gauge consisted of four resistance strain gauges manufactured by TML Co., which formed a full Wheatstone bridge. An Advantech data acquisition (DAQ) card recorded the gauges output values at the sufficiently high rate of 500,000 data points per second. Test specimens were fabricated from two high manganese steels with the chemical compositions presented in Table 1.

Table 1. Chemical compositions of the steels used for the fabrication of torsional specimens (wt. %)

Alloy	C	Mn	Al	Si	Fe
steel 1	0.49	21.6	0.8	2.7	Bal.
steel 2	0.07	20.1	0.6	2.1	Bal.

The geometry of the torsional specimens is demonstrated in Figure 2. In order to prevent sliding between the bars and the specimen, the specimen ends were constructed in the form of hexagonal flanges;

these flanges were installed in hexagonal sockets of the bar ends. Regarding the high work hardening of the investigated steels, in order to increase the dimensional precision, the specimens were fabricated by electrical discharge machining (EDM). The gauge length of the specimens (l_0 in Figure 2) was inversely related to the applied strain rate (see equation (1)). Therefore, to study the influence of the strain rate on the mechanical behavior of the steels, three different gauge lengths of 1, 2, and 3 mm were selected for the specimens.

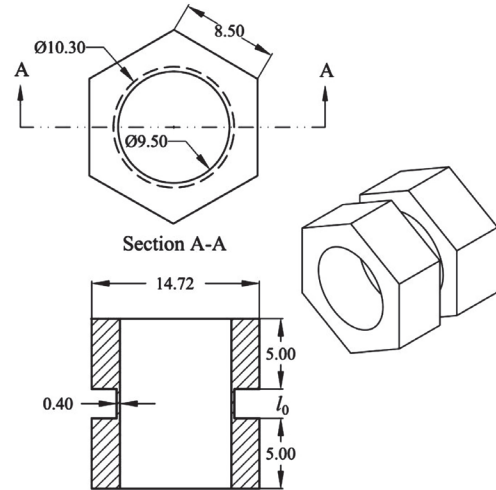


Fig. 2. Geometry of the torsional specimens used in high rate experiments (dimensions in mm).

In order to maintain the working configuration of the testing machine, the incident bar should not be loaded beyond its yield limit. Regarding the mechanical properties of AA6061-T6, which was utilized to construct the bars, by using the Hooke's law for shearing stresses, the maximum allowable angle of twist was calculated to be 27°. In the present work, the angle of twist was set to the safe value of 18°.

The difference between angular velocity of the specimen ends allocated the instantaneous applied strain rate during the test. This difference was directly related to the amplitude of the pulse which was reflected to the incident bar¹⁰. Thus, through equation (1), the applied shear strain rate could be calculated from the reflected strain pulse which was recorded by gauge 1:

$$\dot{\gamma}_s(t) = \frac{2r_s c}{l_0 r_b} \times (-\gamma_R(t)) \quad (1)$$

Where r_s is the mean radius of the thin-walled gauge zone, l_0 is the gauge length, c is the velocity of propagation of the torsional wave along the bars, r_b is the radius of the incident bar, and $\gamma_R(t)$ is the instantaneous amplitude of the reflected pulse. The value of shear strain was calculated by integration of

the shear strain rate from $t=0$ with any desired instance of time:

$$\gamma_s(t) = \int_0^t \dot{\gamma}_s(t) dt \quad (2)$$

The amplitude of the torque which was transmitted to the transmitter bar was the same as that tolerated by the specimen. Thus, the applied shear stress could be calculated as a function of time according to equation (3):

$$\tau_s(t) = G\gamma_T(t) \frac{J_b}{J_s} \frac{r_s}{r_b} = \frac{Gr_b^3}{4r_s^2 t_s} \gamma_T(t) \quad (3)$$

Where J_b and J_s are the polar moments of inertia in the bar and specimen, respectively, $\gamma_T(t)$ is the amplitude of the torsional pulse in the transmitter bar, G is the shear modulus of elasticity, and t_s is the gauge zone thickness. By using equations (2) and (3), the values of shear stress and strain could be calculated at any desired instance of time. Subsequently, by omitting the time from both quantities, curves of shear stress versus shear strain could be plotted. Also, by multiplying the shear stress and dividing the shear strain by $\sqrt{3}$, the true stress-strain curves were obtained.

In order to investigate the influence of pre-straining on the subsequent dynamic experiment, some of the specimens of the low-carbon steel were tested in two stages. Firstly, without activation of the clamps, the incident bar was slowly twisted to the desired angle, and then the strained specimen was used in a dynamic torsional test as described earlier. The twist angle in the pre-straining stage of the tests was selected such that a constant pre-strain of 0.15 was applied to the specimen.

3. Results and Discussion

The true stress-strain curves obtained from the high strain rate torsional tests on steel 1 and 2 (represented in Table 1) are depicted in Figure 3. The flow stresses of steel 2 were obviously higher than those of steel 1 at different strain rates. This was related to the different initial microstructures of the two steels. At ambient temperature, steel 1 had a single phase austenitic structure, while steel 2 had a duplex mixture of epsilon-martensite and austenite. The difference between the flow stresses of the two steels was larger at lower strain rates. This can be attributed to the opposite effects of strain rate on the flow stress of the two steels. The stable room temperature phases of the steels and their microstructural evolutions in the course of straining depend on the stacking fault energy (SFE). Thus, the values of this energy were calculated for both steels using the thermodynamic data available in the

literature ¹¹⁾ and according to the method proposed by Olson and Cohen ¹²⁾. These values for steel 1 and 2 were 32.2 and 4.7 mJ/m², respectively. Therefore, at room temperature, the deformation of steel 1 was expected to take place mainly by mechanical twinning, whereas for steel 2, transformation of austenite to epsilon-martensite occurred as well. However, the high strain rate deformation of a material is accompanied by the phenomenon of adiabatic temperature rise. Depending on the amount of strain and strain rate, deformation of these steels may lead to a temperature rise of up to 150 °C ¹³⁾. On the other hand, it is well established that the stacking fault energy of a high-Mn steel increases as the temperature is increased ¹⁴⁾. Due to the high stacking fault energy of steel 1 prior to the deformation, its SFE exceeded the upper limit value of 35 mJ/m² during the high rate deformation. As a result, its dominant deformation mechanism at high rates of strain was expected to be normal dislocation glide. This is consistent with the strain rate hardening behavior observed for this steel (Figure 3). Decreased dynamic recovery ¹⁵⁾ and the viscous drag effects of solutes ¹⁶⁾ could be suggested to cause such a behavior at high rates of strain. The latter is especially more important at strain rates above 1000 /s.

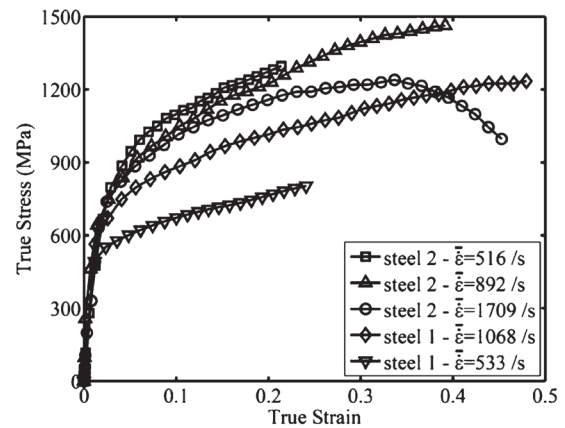


Fig. 3. True strain-strain curves obtained from high strain rate torsional tests.

In contrast to steel 1, the SFE of steel 2 was very low prior to the deformation. Thus, during the high rate deformation, the steel initially was deformed by martensitic transformation. After a certain value of strain was applied, the temperature and hence, the SFE were increased so that the dominant deformation mechanism changed to mechanical twinning. As the strain rate increased, the adiabatic temperature rose and consequently, the flow stress of the steel decreased ⁶⁾. This can be clearly seen in Figure 3. However, the strain rate softening of this steel at small strains (in the vicinity of the yield point) cannot be related to the deformation temperature rise, since this effect is negligible at small values of strain. With an increase

of the strain rate, the impact pressure applied to the test specimen increased. At a particular value of strain rate, this pressure exceeded the critical stress for the nucleation of epsilon-martensite or mechanical twins⁶⁾. As a result, the flow stress at the beginning of the deformation was also decreased with an increase in the strain rate.

The smoothed work hardening rate curves corresponding to high rate deformation of steels 1 and 2 at different strain rates are depicted in Figure 4. The hardening rate for steel 1 was gradually decreased during the deformation. However, in the case of steel 2 at the strain rates of 516 and 892 /s, a higher work hardening rate was observed as compared to that of steel 1.

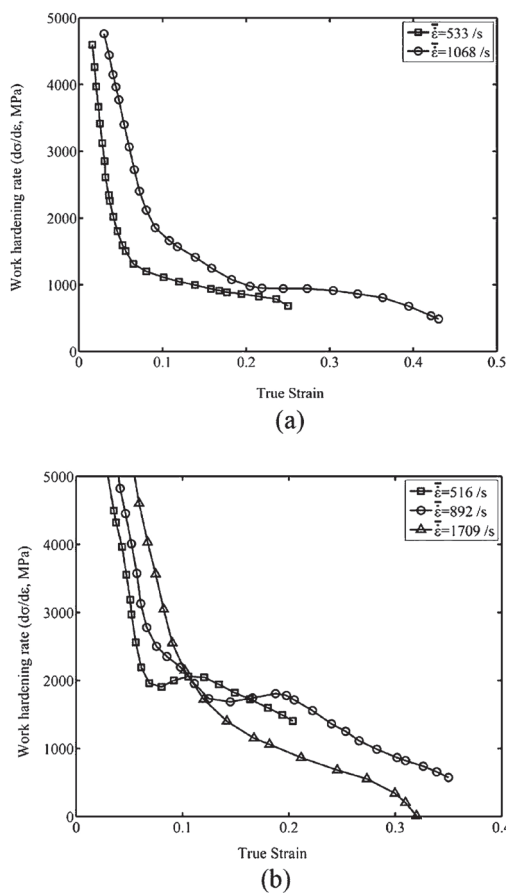


Fig. 4. Work hardening rate in high strain rate torsional testing of (a) steel 1 and (b) steel 2.

Furthermore, the hardening rate was slightly increased at particular values of strain which corresponded to the initiation of mechanical twinning¹⁷⁾. As the average value of strain rate was increased, the pulse duration was decreased. In other words, the amount of time consumed for the application of a certain value of strain was shorter in the test with the higher strain rate (Figure 5). Consistently, the increase of work hardening rate at the strain rate of 892 /s

took place at a larger value of strain when compared to that for 516 /s. This was due to the shorter pulse duration in the experiment with the higher strain rate of 892 /s, as a result of which a larger strain would be required to nucleate twins. However, at the strain rate of 1709 /s, due to minimal pulse duration along with maximal temperature rise, no significant contribution of twinning induced plasticity could be considered. As a result, continuous reduction of the hardening rate continued up to the failure point. Consistently, flow localization occurred for the specimen tested at this strain rate, i.e. 1709 /s (Figure 3).

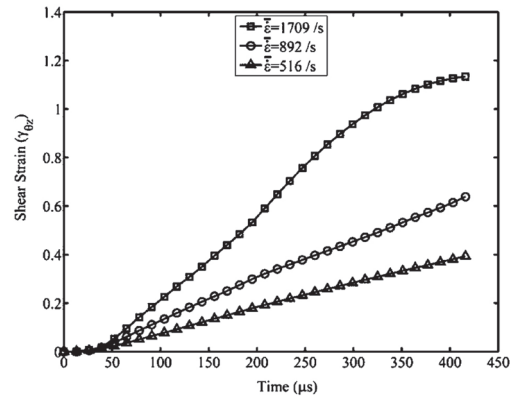


Fig. 5. Shear strain versus time for high strain rate experiments on steel 2.

The hardening rate curves obtained for those specimens of steel 2 which were pre-strained prior to the dynamic torsional experiment are depicted in Figure 6. Only a slight increase of the hardening rate could be observed at certain values of strain, showing that the influence of mechanical twins was noticeably decreased. Regarding the low SFE of steel 2, during the quasi-static pre-straining of the specimens, a considerable fraction of the pre-existing austenite phase was transformed into epsilon-martensite. Therefore, less austenite was available for mechanical twinning during the subsequent high rate deformation of the steel.

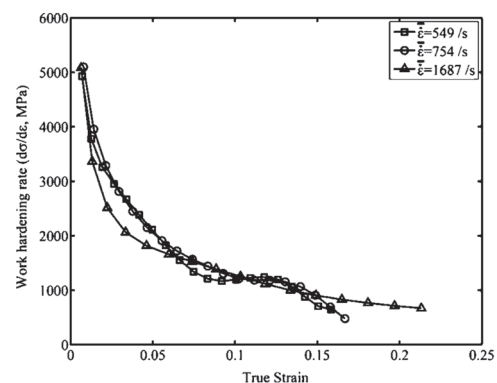


Fig. 6. Work hardening rate in high rate torsional testing of steel 2 after a pre-strain of 0.15.

4. Conclusion

A high strain rate torsional testing machine was designed and constructed. The machine was successfully utilized for dynamic testing of high-Mn steels in the range of strain rates from ~500 to 1700 /s. Normal strain rate hardening behavior was observed for the high-carbon steel, whereas the flow stress of the low-carbon steel was decreased with an increase in the strain rate. Due to the higher stacking fault energy of the high-carbon steel, adiabatic temperature rise led to the intense reduction of the work hardening rate in this steel. In contrast, mechanical twinning effectively increased the hardening rate for the low-carbon steel up to the strain rate of ~900 /s. Additionally, it was observed that quasi-static pre-straining of the low-carbon steel decreased the contribution of mechanical twins to the work hardening behavior of this steel in the subsequent dynamic deformation.

References

- [1] Y. Li, Z. Lin, A. Jiang and G. Chen: *Mater. Des.*, 24(2003), 177.
- [2] J. Hopkinson: *Original Papers by J. Hopkinson*, Vol. 2, At the University Press, Cambridge, (1901), 316.
- [3] H. Kolsky: *Proc. Phys. Soc.*, 62(1949), 676.
- [4] J. Harding, E.O. Wood and J.D. Campbell: *J. Mech. Eng. Sci.*, 2(1960), 88.
- [5] W.W. Baker and C.H. Yew: *J. Appl. Mech.*, 33(1966), 917.
- [6] Z. Xiong, X. Ren, W. Bao, S. Li and H. Qu: *Mater. Sci. Eng. A*, 530(2011), 426.
- [7] D.B. Santos, A.A. Saleh, A. Azdiar, A. Carman, D.M. Duarte, E.A.S. Ribeiro, B.M. Gonzalez, E.V. Pereloma: *Mater. Sci. Eng. A*, 528(2011), 3545.
- [8] G. Dini, A. Najafizadeh, R. Ueji and S.M. Monir-Vaghefi: *Mater. Des.*, 31(2010), 3395.
- [9] O. Bouaziz, S. Allain, C.P. Scott, P. Cugy and D. Barbier: *Curr. Opin. Solid State Mater. Sci.*, 15(2011), 141.
- [10] A. Gilat: *Torsional Kolsky Bar Testing, Mechanical Testing*, Vol. 8, ASM Handbook, Materials Park, ASM International, (2000), 1134.
- [11] A. Dumay, J.P. Chateau, S. Allain, S. Migot and O. Bouaziz: *Mater. Sci. Eng. A*, 483-484(2008), 184.
- [12] G.B. Olson and M. Cohen: *Metall. Mater. Trans. A*, 7(1976), 1897.
- [13] A. Khosravifard, M.M. Moshksar, R. Ebrahimi: *Mater. Des.*, 52(2013), 495.
- [14] A. Imandoust, A. Zarei-Hanzaki, M. Sabet and H.R. Abedi: *Mater. Des.*, 40(2012), 556.
- [15] F. Huang and N.R. Tao: *J. Mater. Sci. Technol.*, 27(2011), 1.
- [16] S. Curtze and V.T. Kuokkala: *Acta Mater.*, 58(2010), 5129.
- [17] D. Barbier, N. Gey, S. Allain, N. Bozzolo and M. Humbert: *Mater. Sci. Eng. A*, 500(2009) 196.